

On the Design of an Analog-Dyadic Converter CRN

Mathieu Hemery^[0000-0003-2963-7067]

Inria Saclay Ile de France, EPI Lifeware, Palaiseau, France

Abstract. The Chemical Reaction Networks (CRN) interpreted through the differential semantics, even when restricted to elementary reactions with mass action law kinetics, form a Turing-complete language. This means that any computable real function can thus be programmed, and in fact compiled, in an abstract CRN that will compute it with an arbitrarily high precision. In this computational framework, the information carriers are the molecular concentrations, the required precision is given as input, and the output concentration is guaranteed to satisfy the required precision. On the other hand, one can be interested in estimating the derivative of an unknown input signal or in reading the concentration value of an input molecular species. By nature, such problems can only be approximated with a finite precision. Hence, the computation framework proposed previously cannot be applied and we need to design and analyze custom CRNs to perform these tasks. In this paper, we present an analog-dyadic converter CRN which takes as input one molecular concentration (in $[0, 1]$ but not necessarily computable), and produces as output a sequence of “on” and “off” spikes corresponding to some extent to the sequence of bits in the dyadic representation of the input concentration. We provide a detailed analysis of the source of errors and their behavior when varying the reactions rate constants. We conclude by sketching a possible design for a reader module that takes as input an arbitrary concentration and a desired precision and outputs a dyadic encoding approximating the value of the concentration with the desired precision. We leave as an open question to prove the correctness of our construction.

1 Introduction

Turing machine is a concrete, albeit unpractical, model for the theoretical study of computers’ possibilities. A computer being any machine able to perform calculations [14]. Its interest resides in its simplicity as it is composed of one or several infinite tapes, a head, a finite set of symbols to be written on these tapes and a finite set of rules. Despite this sobriety, the Church-Turing thesis states that Turing machine is one form of the universal computer in the sense that any function that can be computed by a computer of any sort can also be computed by it.

A less known ancestor of mechanical computing is the integrating machine of James Thomson (the brother of Lord Kelvin) [13] which later became the

differential analyzer and the *General Purpose Analog Computer* (GPAC) with the work of Shannon [12] and others. The central idea in *analog computing* is to represent the mathematical values of the computation through physical quantities, be it electrical or mechanical ones, and perform operations on them through the physical manipulation of these quantities. The idea, at this time, was mainly to reproduce the behavior of the model of interest by building a more convenient analog system obeying the same laws and then perform measurements directly on this “maquette”. While very efficient, particularly in terms of energy expenditure, this framework is also limited in its representative power. Indeed, the solutions that can be *generated* by such a machine are necessarily constrained by their physical embodiment. In particular, they are always analytic[3], which seems to exclude GPAC as a model equivalent to Turing machine.

However, in [7] and [1], Graça, Bournez *et al.* realize the *tour de force* to show that GPAC and thus Polynomial Ordinary Differential Equation (PODE) can have the same expressing power as a Turing machine and are thus a Turing complete framework. The central idea was to consider that the function represented by the machine with variables \mathbf{x} is not the relation: $t \mapsto \mathbf{x}$ – where the function is generated by the machine – but $\mathbf{x}(t=0) \mapsto \lim_{t \rightarrow \infty} \mathbf{x}(t)$ – where the function is computed at the limit. This is significant because PODE is a purely mathematical notion. If the Church-Turing thesis is correct, it implies that the computational power of any physical machine may be defined through a purely mathematical setting.

Building upon these works, our team has shown that through the differential semantics, chemical reaction networks (CRN) can implement arbitrary PODE and are thus also a Turing complete framework able to perform any computation [6]. These results drive us to study the theoretical and practical aspects of CRN seen as a programming language. This leads us to propose a complete pipeline that compile mathematical functions to elementary CRN [5] and to study the theoretical aspect of the intermediate operation of quadratization [9].

A natural question that is both theoretically interesting and practically relevant is the method used to read the result of the computation once the machine has reached the desired precision. It is to shed some light on this aspect that we propose the present paper.

We present here an analog-dyadic converter that relies entirely on elementary reactions of chemical species. We take great care to propose an implementation that uses as few species and reactions as possible while still performing its function with accuracy and robustness. The main idea is to receive the concentration of a species as input and display a sequence of binary spikes that represents the encoding of the initial concentration as a dyadic number. Hence, allowing a “physical observation” of the initial concentration value with increasing precision as the number of spikes increases.

From a more theoretical point of view, this constitutes a central and non-trivial part of the realization of an analog computer, be it with CRN or PODE. Indeed, the possibility to compute a quantity is of no use if we cannot read the result. But given the undecidability of the comparison, it is not evident that this

task is actually possible. A careful analysis shows that our device can only reach a certain precision that depend upon the rate constants and the initial input. This validity domain exhibits a fractal pattern. Fortunately, by tuning the rate constants, it seems possible to expand the validity domain and reach an arbitrary precision, hence allowing us to build a reader module that complete the computation module of [6]. To complete the proof of the correctness for the full construction, we would need a careful analysis of the clock – and its interrelation with the other parts of the CRN – and of the halter module.

Finally, this work is also an attempted step toward the study of the Hartmanis-Stearns conjecture formulated in 1965 and still pending [8]. This conjecture posits that only the rational or transcendental numbers can be computed in real time, in the sense that for a real x , there exists a multi-tape Turing machine taking p as input and returning as output a rational r approximating x with a precision 2^{-p} in a time $O(p)$.

Interestingly, the simple CRN:



is such that X converges exponentially fast toward the irrational but algebraic number $\sqrt{5}$. It is “simply” a matter of retrieving this information. We will see at the end of this article that this is possible with a PODE either with bounded concentrations and a time scaling like $o(p^2)$ or with concentration and time scaling like $o(p)$. Hence, the Hartmanis-Stearns conjecture reduces to: “How can we relate the time of a bounded PODE to the one of a multi-tape Turing machine?”

The plan of this article is the following. First, we will remind the main mathematical tools and aspects needed to understand the notion of CRN and the dyadic representation of numbers, thus setting the notations. We will then present the functioning of the converter and explain the different elements that allow it to perform its function in a robust way. After that, we will perform an-in depth analysis of the main causes of precision loss in order to determine what is the expected precision and how it scales with the different parameters of the model. We finally use this analysis to show how to alter this device to produce a reader module, completing the computation framework of Fages et al.

2 Notation and computation framework

2.1 Chemical Reaction Network

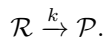
Chemical Reaction Network is a well-established framework used by chemists and biologists to represent the interactions of chemical components and study the various behaviors and properties that emerge from these interactions.

Formally, a CRN is given as a set of species and a set of reactions. These reactions are tuples composed of two multisets of species, the reactants \mathcal{R} and the products \mathcal{P} , and a function f indicating the rate at which the reaction takes place.

Once a CRN is provided, it is possible to interpret it using several semantics: boolean, stochastic, differential, etc. It is this flexibility that gives CRN its modeling power, as the same description may be used through a great variety of tools coming from various domains of science.

In this paper, we will only use the *differential semantics* that consists in deriving a set of ordinary differential equations (ODE) from the CRN. For each species, we attribute a variable representing its concentration and build its derivative by collecting the rates of each reaction in which it participates and multiply it by its signed stoichiometric coefficient (its index in the multiset of products minus its index in the one of reactants).

We moreover restrict ourselves to *Mass Action Law* where rate functions are parameterized by a single positive number k (the rate constant) and are given by the product of the concentrations of all its reactants multiplied by the constant k . In this case, we obtain Polynomial ODE (PODE). We will use the standard notation with an arrow going from reactants to products and an upper index indicating the rate constant if it is different from one:



The differential semantics provides a canonical mapping from CRN to ODE that uniquely associates a set of differential equations to each CRN. For example, the CRN: $A + B \xrightarrow{k} A + 2C$ is associated to the PODE

$$\dot{A} = 0, \quad \dot{B} = -kAB, \quad \dot{C} = +2kAB. \quad (2)$$

A natural question is then: does there exist an inverse mapping? And the answer is: yes, but!

Yes, for any ODE \mathcal{E} that uses only elementary mathematical functions, we can construct a CRN such that a subset of the variables of its associated ODE through the canonical mapping exactly admits the same solution as \mathcal{E} [11]. For mathematical variables A that may be negative, it is possible to split them between their positive (A_p) and negative (A_n) parts and build a CRN for which the observable $A_p - A_n$ will exactly follow the initial ODE \mathcal{E} [6,10]. But, this mapping is not canonical and there is quite a lot of play for the “implementation” of a particular ODE. This is both a curse, because it gives us a lot of arbitrary choices to make in order to provide a particular CRN, and a boon, because it allows us to add additional constraints that may bring us desirable properties upon the constructed CRN.

We study Mass Action Law for two reasons. First, it emerges quite naturally from collision theory, making them “more elementary” than other rate functions. These are indeed often coarse-grained approximations of the behavior of more complex Mass Action Law CRN (see [15] for a historical review on Mass Action kinetics). More surprisingly, it has been shown that Mass Action Law CRNs interpreted through the differential semantic are Turing complete in the following sense[6]:

Theorem 1. *For any computable function $f : \mathbb{R}^k \rightarrow \mathbb{R}$, there exist a finite CRN with mass action law kinetics, over a set of species S_i and a polynomial function p such that, if $S_i(t = 0) = p(x)$, then the unique solution of the differential semantics interpretation of the CRN is such that*

$$\forall t > 1, |S_1(t) - f(x)| < S_2(t), \lim_{t \rightarrow \infty} S_2(t) = 0.$$

Said otherwise, for any computable function, we can construct a CRN over a finite number of species that encodes the input upon the initial concentration of its constituent species, and output the result of the computation as the concentration of the first species at the end of time while also providing a bound on the error on the second species.

It is here natural to ask how, at the end of the computation, we can read the result encoded in the concentration of a chemical species? This is precisely the question that motivates this paper and for that we will need to introduce the notion of dyadic number.

2.2 Dyadic notation

The set of dyadic numbers denoted \mathbb{D} is the one of numbers that can be expressed as a fraction whose denominator is a power of two, that is:

$$\mathbb{D} = \left\{ x \mid \exists n, p \in \mathbb{Z} \times \mathbb{N}, x = \frac{n}{2^p} \right\}.$$

It is a subset of the rational numbers.

By construction, a dyadic number have a natural finite representation which is the binary equivalent of decimal, for u and d the largest and smallest needed powers: $x = \sum_{p=d}^u b_p 2^p$, where $b_p \in \{0, 1\}$ and of course, u and d can both be positive or negative.

For example:

$$\begin{aligned} 1.8984375 &= 1 + \frac{1}{2} + \frac{1}{4} + \frac{1}{8} + \frac{0}{16} + \frac{0}{32} + \frac{1}{64} + \frac{1}{128} \\ &= 1.1110011_2 \end{aligned} \tag{3}$$

It is easy to see that \mathbb{D} is dense in \mathbb{R} in the same way that the rationals or the decimals are. As for the decimals, a real number always has at least one (possibly infinite) dyadic representation. They are thus a convenient set to represent real numbers in a framework where the number of symbols in the numeration system is scarce, the same way that binary allows representing integers with only two symbols.

We now have all the elements to present the basic structure of our converter.

3 The analog-dyadic converter

The purpose of the dyadic converter is, starting from a species, the concentration of which is between 0 and 1, to “write” the dyadic representation of this initial

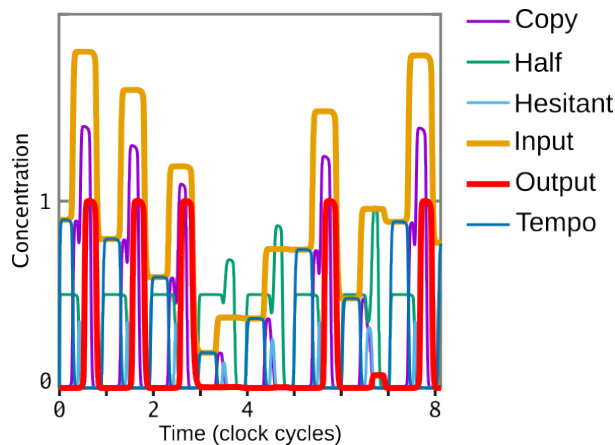


Fig. 1. Time course of the dyadic converter through 8 complete cycles of the clock. During the k th cycle, the *Output* species (in bold red) spikes or not according to the comparison of the *Input* species (in bold orange) to a threshold species. Here we can see that the output is 11100101. Note that this is different from the expected result as, $\text{Input}(t = 0) = 0.9 = 0.11100110\dots_2$. The 6 first bits are correct, but we suffer from an error on the 7th one. The cause of these errors, and how to mitigate them, will be discussed in this paper.

concentration as a sequence of binary spikes in the concentration of one species (here named “Output”). An example of this behavior is shown in Figure 1.

The main idea is simply to follow the same steps as those of the typical algorithm used to convert a number to its dyadic representation. In a nutshell, we first compare the current value of the input to one half and write a one or a zero accordingly. Then, in order to pass to the next bit, we need to zoom in. This can be done by doubling the input and subtracting one if necessary to keep it between 0 and 1. Then we loop.

The reactions of the dyadic converter are a bit more involved as they include ancillary species to perform the function with the constraints of chemical implementation. The pseudocode along with its CRN implementation is given in table 1.

3.1 Overview

Our conversion module is composed of five interacting parts: a clock, a copy, a comparison, a subtraction and a cleaning mechanism.

The purpose of the clock is to play the role of a musical director. It coordinates all the other reactions as they should be activated in order to correctly perform the desired behavior. This is achieved by having a set of species that alternate active and passive phases in a predefined order and use them to catalyze all the reactions of the other parts.

	Pseudocode	CRN
Copy	$Copy := Input$	$Input \rightarrow Input + Tempo$
&	$Input := 2 * Input$	$Tempo \rightarrow \emptyset$
Doubling		$Tempo \rightarrow Copy + Input$
	$Half := \frac{1}{2}$	$\emptyset \rightarrow Half, Half \xrightarrow{2} \emptyset$
Comparison	$Half := 0$ if $Half < Copy$	$Copy + Half \rightarrow 2Hesitant$
	$Copy := 0$ if $Half > Copy$	$Hesitant + Half \rightarrow 2Half$
		$Hesitant + Copy \rightarrow 2Copy$
Spiking	$Output := 1$ if $Copy$	$Copy + Inactive \leftrightarrow Copy + Output$
Subtraction	$Input := Input - Output$	$Output + Input \rightarrow Inactive$

Table 1. Description of the operations performed by the dyadic converter module given with a pseudocode representation along with the CRN implementation. For clarity, the clock and its regulation are not represented here. The exact model is given in (9).

The copy reactions allow us two different effects. First, it creates a copy of the input that can be destroyed during the comparison step without losing the value of the input that should be passed (up to some modifications) from one cycle to the next. It also allows us to double the value of the input.

The comparison scheme is based upon the classical mechanism of *approximate majority* [4]. It compares with good precision the value of the Copy to a predefined threshold, here: one half. While a more simple comparison could have been implemented with a simple bidegradation, the approximate majority scheme is here preferred for its robustness and the strength of its signal. Indeed, at the end of the computation the reminding species is always higher than one half, hence ensuring an easy reading. Of course, this mechanism is not perfect, and it takes time to discriminate, especially between close concentrations, a phenomenon that is the core of section 4.2.

The subtraction reaction is a simple bidegradation. It relies on an output species that is activated if and only if the input is higher than one half based on the result of the previous comparison mechanism. This has two benefits: first, it creates a robust output signal that is simply 0 or 1. Second, as it goes to 1 independently of its previous value, it provides us with the unitary value that should be subtracted from the input to start the next cycle of the dyadic conversion as explained in the pseudocode.

The cleaning reactions finally simply remove the intermediate species in order to start the next cycle with null concentration. This step is facultative as these species are set by the different reactions to their desired values independently of their initial concentrations. However, cleaning them ease the analysis of the model.

We will now take a bit more time to present in detail the two more involved elements of the CRN, namely the clock and the comparison module.

3.2 Clock

It is now known for some time that you can easily generate a sine and cosine with 4 species and 6 reactions [6]. In this CRN, the 4 species are the positive and negative parts of the trigonometric functions while the reactions are, for four of them, the catalytic production of the next species, the two others being bidegradations of the positive and negative parts.

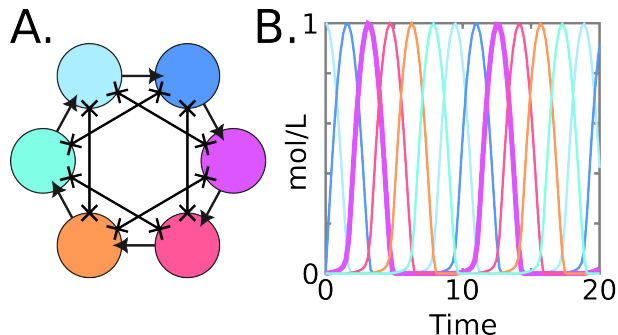
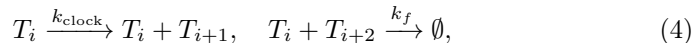


Fig. 2. **A.** Schematic representation of a six-step clock. Each species activates the next one and participates in a bidegradation (here depicted as a two crossed connector) with its second neighbor. **B.** The time course of the CRN presented in panel A. with corresponding colors. Activations have rates $k_{\text{clock}} = 1$ while degradations have rates $k_f = 1000$. At $t = 0$ one of the species (here light blue) has an initial concentration of 1. The violet species has been highlighted only to ease the readability of the behavior of a single species.

Surprisingly and as presented in Figure 2, this is not limited to 4 species. For any $n \geq 4$, the CRN:



where the indices $i \in [1, n]$ and should be understood modulo n and the rate k_f is high enough to ensure that bidegradations strongly dominate other reactions, also exhibits an oscillatory behavior. Even more beautiful, it gives us an n -clock where all the species alternates between an "active" sinusoidal behavior corresponding to one "bump" and a "dormant" null behavior where it simply waits to be activated again.

By using each of these species as a catalyst for other reactions, we can associate a part of the CRN of table 1 to a particular time of the n -clock, the same way the circadian clock regulates the activity of pathways in cells.

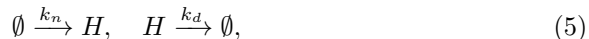
For a computer scientist, our clock is thus of a surprising kind as one complete cycle of the clock does not correspond to one elementary operation of the system – as it would in a traditional computer with a clock used for synchronizing the different parts – but to a full cycle of operations leading to the computation of one bit of the dyadic encoding.

For a perfect computation, the steps of the conversion should be performed sequentially and independently. The main problem is that our clock is such that two consecutive species, T_i and T_{i+1} display a strong overlap, as can be seen in Figure 2. Even the overlap between T_i and T_{i+2} may be too important when strong guarantees are needed: typically when the two steps are likely to create a positive feedback loop that may lead to an exponential divergence as is the case for the two reactions of the copy mechanism: $Input \rightarrow Input + Tempo$ and $Tempo \rightarrow Copy + Input$. To avoid that, we can always let more steps of the clock pass between such reactions. We may also increase the rate constant k_f as it helps to soothe this unwanted overlap.

As this work is also a proof of principle for a short device, we try to minimize the use of such insulation mechanisms to keep our device as streamlined as possible. In the context of a formal derivation of the theoretical possibility of CRN computation, we would take $n = 80$ and associate the different step to $T_{10 \cdot i}$ instead of T_i to ensure strong insulation.

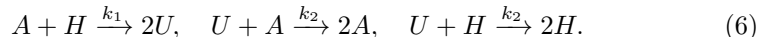
3.3 Thresholding with Approximate Majority

The comparison relies first on the production of a threshold species (H for Half):



that will converge to the ratio: $\frac{k_n}{k_d}$. In our case, we use $k_d = 2k_n$ to obtain a one half ratio. This step is performed as an initialization and realized during the first step of the clock.

Then during step 5, an approximate majority scheme is performed where the species of interest A^1 is compared to the H species through the formation of an undecided U species:



In model (9), we set $k_1 = k_2 = k_{AM} = 10$. We keep them different here for the analysis.

The differential semantics of this reaction system gives us the following ODE:

$$\begin{aligned} \dot{A} &= -k_1AH + k_2UA, \\ \dot{H} &= -k_1AH + k_2UH, \\ \dot{U} &= 2k_1AH - k_2U(A + H). \end{aligned} \quad (7)$$

The approximate majority is well known to converge to a steady state where the species that was initially the more abundant between A and H will be the

¹ To avoid cluttering the notation of this section, we use A and a for the study of the approximate majority in its own. In the full CRN, the species to be compared will be *Copy*. Similarly, the undecided U species is named *Hesitant* in the full CRN.

only one remaining with a concentration equal to the sum of the two initial ones. That is, we have when $t \rightarrow \infty$:

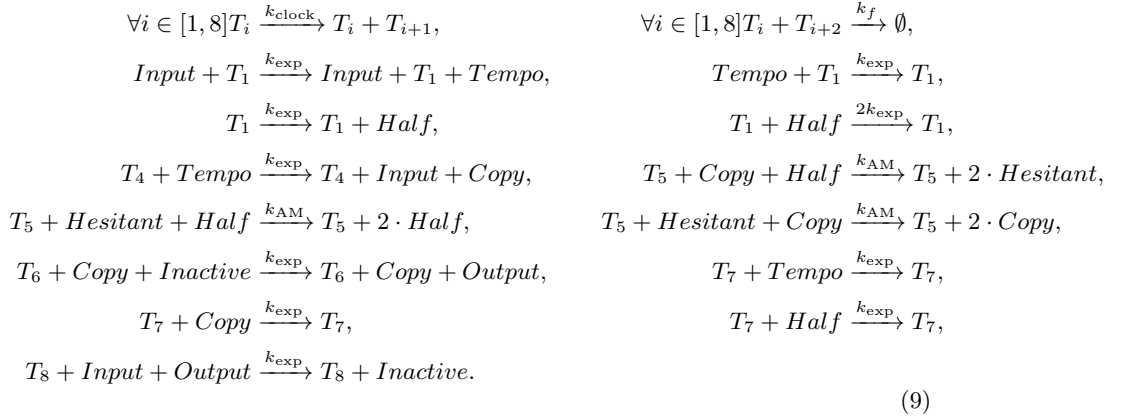
$$\begin{cases} A = A_0 + H_0, & H = 0 & \text{if } A_0 > H_0, \\ A = A_0, & H = H_0 & \text{if } A_0 = H_0, \\ A = 0, & H = A_0 + H_0 & \text{if } A_0 < H_0. \end{cases} \quad (8)$$

Using this scheme, we can thus test if the initial concentration of A was below or above the threshold H just by testing its presence at the end of the process. This supposes, that the approximate majority dynamic had enough time to converge. Or at least that, if it should be 0, the eventual traces of the A species are low enough to remain undetected. This question will be treated in length in section 4.2.

Now that we have presented all the elements, let us see how they perform together.

3.4 Dyadic converter

The full CRN of our converter is given by:



With the initial condition: $T_1 = 1, \text{Inactive} = 1$ and of course $\text{Input} = I_0$. For this paper, we set: $k_{\text{clock}} = 1, k_{\text{AM}} = k_{\text{exp}} = 10, k_f = 1000$.

In Figure 3, we illustrate the behavior of the model through one full cycle of the clock depending on whether I_0 , the initial value of the input, is below or above the threshold of $\frac{1}{2}$ and thus whether the output species should spike or not. We can see that at the end of step 4, the *Copy* species now has the value I_0 and *Input* itself has doubled its value. Then the *Copy* is compared to *Half* and thus set back to 0 in the first case, while it goes to $\frac{1}{2} + I_0$ in the second one. The presence or absence of *Copy* at this time activates (or not) the production of *Output* to its target value of 1. It is this unitary (or null) value which is then subtracted to the current value of *Input* to set it to its value for the next iteration of the clock, that is either $2I_0$ or $2I_0 - 1$.

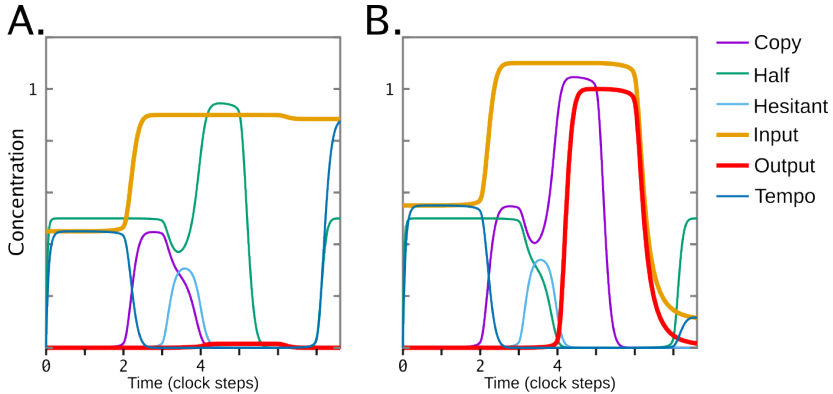


Fig. 3. Numerical integration of one full cycle of the clock for two different initial conditions. One where the *Input* species is slightly below (**A.**) the $\frac{1}{2}$ threshold and one where it is slightly above (**B.**).

We just show that our simple CRN is able to display the desired behavior by implementing the pseudocode of table 1 to output at least the first bit of the dyadic encoding of its input. We have also seen that this network is susceptible of making mistakes. After a certain time, the initial precision is lost and the bits no longer correspond to the exact representation. We call *precision* the number of correct bits that the CRN is able to output. This quantity depends on the parameters of the CRN and the value of the initial input.

We will now take time to determine what are the main sources of such discrepancies and how we can control them. We will thus determine the influence of the parameters of the CRN on these errors and give some theoretical bounds upon the precision of our conversion device.

In particular, we will estimate the validity domain of our device. Indeed, we have seen that the precision we can achieve depends on both the input and the rate constants. For a given set of parameters $(k_{\text{clock}}, k_{\text{exp}}, k_{\text{AM}}, k_f)$, it is this attainable precision as a function of the input that we want to determine.

4 Detailed analysis

Our analysis of the errors relies on three properties:

- Converging exponential have had enough time to reach a precision ϵ with respect to their target value during one step of the clock (see section 4.1 but also appendix A.3).
- The different steps of the clock are well separated. This avoids any leakage between successive steps. While this is only approximately the case for our 8-clock example, we can increase the size of the clock to ensure perfect insulation.

- The Approximate Majority mechanism had enough time to discriminate between its two constituents up to a precision δ^* (see section 4.2 and appendix A.2).

Conceptually, the two first properties may be thought as the use of a perfect clock where the pieces of cosine have been replaced by rectangular signals of amplitude 1 and duration τ . Hence, the different parts of the module are activated at full intensity for a constant duration before being switched off. For this reason, we rely on the parameter τ as a convenient parameter to describe the clock. As shown in appendix A.3, we have the relation $\tau = \frac{2}{k_{\text{clock}}}$.

For the last property, we will see that it creates a constraint on the different rate constants of the reactions.

4.1 Premature halting

The main culprit in terms of error is the premature halting of the reactions before they reach their asymptotic steady states. Note that this error is unavoidable as the exact computation is only performed in infinite time due to the framework of “computation at the limit”.

Most differential equations involved in the dyadic converter harbor converging exponential with a rate k_{exp} as solutions. Knowing this allows us to compute the bounds on the value of the different species during the time evolution of one cycle of our converter module as a function of the input value I_0 . This allows us to bound I_f the value of *Input* at the end of the clock cycle (the full detail of this derivation is given in appendix A.1):

$$\begin{cases} I_f \in [2I_0 - 3\epsilon, 2I_0] & \text{if } I_0 < \frac{1}{2}, \\ I_f \in [2I_0 - 1 - 2\epsilon, 2I_0 - 1 + \epsilon] & \text{if } I_0 > \frac{1}{2}. \end{cases} \quad (10)$$

An error of order 3ϵ after each cycle means that the value of the Input after n cycles has accumulated an error like:

$$e_n = 3(2^n - 1)\epsilon.$$

Thus if we still want a good precision at step p , this means that we want $3 \cdot 2^p \epsilon \ll 1$ and for this, we have to impose: $k_{\text{exp}}\tau \gg p$.

Reaching the p th cycle asks for a time $T(p) \propto \tau p$, and as we have $\tau \propto p$ by our previous computation, we conclude that reaching a given precision asks for a time that scales quadratically:

$$T(p) \propto \frac{p^2}{k_{\text{exp}}}. \quad (11)$$

However, the premature halting of the converging exponential is not the only cause of errors that can be perpetrated by our converter. The other main cause of errors being the incapacity to distinguish between two similar concentrations when the input and threshold species are too close, that is, when the input is near one half and this is what we discuss in the next section.

4.2 Comparison

Analyzing the ODEs of the approximate majority 6, (see appendix A.2 for the full derivation), we deduce that the system does not have the time to reach a proper convergence when the initial value is too close from one half. Introducing $\delta \geq 0$ as $I_0 = \frac{1}{2} \pm \delta$ we can derive that when $k_1 \gg k_2$, there exists a threshold δ^* given by:

$$\log(\delta^*) = -\frac{\log(4r^2)}{1 + \sqrt{2}} - \frac{k_2\tau}{1 + \sqrt{2}} \quad (12)$$

such that starting with a lower value for δ indicates that the approximate majority mechanism will at time τ be in a state where the species that should be close to 0 is actually higher than r . For ensuring the bounds of the previous section, we need $r < \frac{\epsilon}{\tau k_{\text{exp}}}$. Note that this relation introduce a dependency between the error sources, lowering ϵ also lower r which leads to higher δ^* .

When $\delta < \delta^*$ the comparison mechanism will not have the time to converge properly, this removes $[\frac{1}{2} - \delta^*, \frac{1}{2} + \delta^*]$ from the validity domain for precision 1. During the next cycle, the same phenomenon appears, creating two new forbidden intervals: $[\frac{1}{4} - \frac{\delta^*}{2}, \frac{1}{4} + \frac{\delta^*}{2}]$ and $[\frac{3}{4} - \frac{\delta^*}{2}, \frac{3}{4} + \frac{\delta^*}{2}]$ for the precision 2. And the same process repeats at each clock cycle, creating the fractal pattern of the validity domain represented in black in Figure 4 A. For this picture, we choose: $\delta^* = e^{-\frac{10.1}{3}} \simeq 0.036$.

To conclude on the behavior of the approximate majority scheme, it has to be said that with a finite number of molecules, the stochastic aspect of this CRN would also impose some limit. We would have to set a limit on fault tolerance: "I want my discrimination to be correct in at least 99% of the cases" and this would translate into a new limit δ_{stoch} with a behavior similar to δ^* , effectively setting a limit to how far we could lower δ^* .

Now let us check if these theoretical considerations are valid once we start making numerical simulations of our device.

4.3 In practice

To evaluate the actual quality of the response, we perform extensive numerical simulations, always using model (9) for 1000 different values of the initial input in the range $[0, 1]$. We then automatically extract the presence or absence of the 10 first spikes² recovering to the effective encoding (which may be different from the mathematical exact one).

We propose two different measures to determine the precision of our model:

² For this analysis, we consider a spike to be present if the Output species spikes above a threshold of $\frac{1}{3}$ thus making a pessimist assumption about the ability of the reader to discriminate intermediate value. It could be interesting to add an *unclear* state for these intermediate values and see how this allows to catch the precision loss of the module.

- The *precision* defined as the first bit where the model makes an error (depicted in red in fig.4A.),
- The *error* defined as the signed difference between the actual number and the number encoded by the dyadic representation output by the model (see fig.4B).

For example, in the simulation presented in Figure 1, the input is $0.9 = 0.1110011001100\dots_2$ and the output of the model is $0.11100101\dots_2 = 0.8945$. In this case, the precision is 7 and the error is -0.0055 .

Precision and *error* are two different measures and a low precision is only a piece of evidence for a high error. Think of 0.500002 and 0.49995 which differ very slightly despite a difference as early as the first digit. It is thus important for us to look at both.

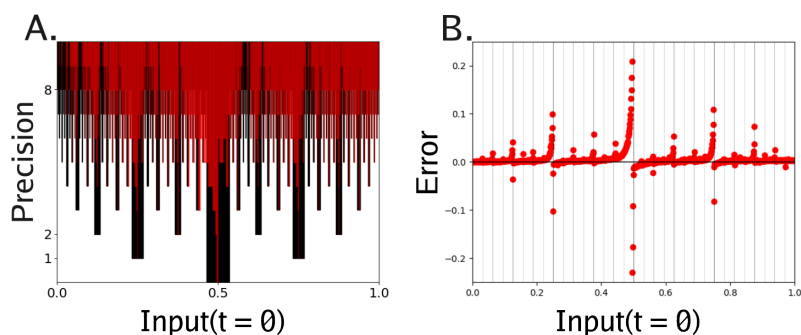


Fig. 4. Analysis of the actual behavior of the converter module for $k_{\text{clock}} = 1$ and $k_{\text{exp}} = k_{\text{AM}} = 10$ and 1000 different values of the input between 0 and 1. The system is then numerically integrated, and the spikes are automatically detected to determine the system response over 10 full cycles of the clock. **A.** Comparison between the theoretical precision of the approximate majority analysis (in black) and the actual precision of the full CRN as measured after numerical integration (in red). **B.** *Error* of the dyadic converter as a function of the initial input.

We can see on the panel **A.** that the actual precision is more subtle than the theoretical picture presented in black. This is because of the presence of errors due to premature halting but also due to our choice to present a streamlined CRN with as few reactions as possible and to take low values for the rate constants. This allows us to show explicitly the behavior of our converter in its different error regimes.

First, it needs to be emphasized that both panels in Figure 4 exhibit the fractal pattern discussed above. Moreover and as expected, the precision is essentially bounded by the results of our AM analysis. We also see that the effect of premature halting is more important for high values of the input, explaining the lower precision near 1. (This is also true for error, but is difficult to see due to the scale of the figure.)

Let us now discuss briefly the behaviors of the CRN that were not covered by our previous analysis. To derive our computation, we tried to estimate a lower bound on precision and rely on two hypotheses: first, a pessimistic approach to the error, since as soon as the parameter δ was below the critical threshold, we consider the system to be faulty, and second, an exact value for the quantity to be compared. Sadly, both assumptions are false.

Manifestly, errors are not ineluctable inside this black region, but being too close to $\frac{1}{2}$ indeed incurs a loss of precision as the system is halted before it reaches consensus. First, we can see that the error is the worst slightly below one half. This comes from the fact that the Half species we compare to suffer from the premature convergence effect discussed in 4.1. For this set of parameters, the actual threshold seems to be around 0.496.

The way the approximate majority errors affect the result is also interesting. Indeed, due to the continuous nature of our computation, around one half, it is possible to see “aborted” spikes of the Output that are neither 0 nor 1. This kind of behavior can be seen around time 80 in Figure 1. Through the subtraction part, this error propagates to the Input species meaning that the next cycle start with an incorrect input.

Typically, just after the one half threshold, we would expect the input species to be close to zero at the beginning of the second clock cycle. If this was the case, we would only get zeros after that, and so, a low error. But as can be seen on panel **B.**, it is not the case. This creates the hyperbolic pattern that appears around one half and, by the fractal pattern mentioned before, around all dyadic numbers with a low denominator as indicated by the black vertical lines.

Let us now talk about the scaling of these errors with the different rates of our model. Amusingly, the responses of the system to a tuning of the different rates are not independent. While we would have thought that a large increase in k_{exp} without modifying k_{AM} would reduce the source of error to only the problematic cases around one half – and its fractal successors – it is not what actually happens. Indeed, a high k_{exp} makes the spiking reaction so sensitive, that even a residual fraction of the Copy species is detected and trigger the spike as revealed in equation 12.

Conversely, increasing only k_{AM} effectively narrows the problematic fractal region by decreasing δ^* until the precision is essentially limited by the problem of premature halting. Hence, effectively increasing the precision necessitates to increase k_{exp} while keeping $k_{\text{AM}} \gg k_{\text{exp}}$.

All this can be used to build a *reader* module, completing the computation module of Fages et al.

4.4 Building a reader module

Theorem 1 ensures that for any computable function f , we can build a CRN on species \mathbf{S} such that for any x , the first species converges to $S_1 \rightarrow f(x)$ and the second species, which is positive, decreases and converges to 0, controls the error: $|S_1 - f(x)| < S_2$. For a desired precision ϵ we can wait until $S_2(t^*) = \frac{\epsilon}{2}$

and return any value past this point in time. We choose to stop the computing device at a particular time $t \geq t^*$ and denote $\tilde{f}(x) = S_1(t)$. Then you need to start the reading device. A prototype of linker CRN is presented in appendix A.4 that allows to let the computing CRN converge before halting it and starting the reader module.

The difficulty is that $\tilde{f}(x)$ is *a priori*, an ordinary real. There is no reason why it should be computable. We only know that it approaches the result with the aforementioned precision. Starting from the converter CRN, we can build a reader module that takes this value as input along with the precision ϵ and produces an observable behavior allowing the user to construct a dyadic number d such that $|d - \tilde{f}(x)| \leq \frac{\epsilon}{2}$. Hence, we have with d a dyadic approaching $f(x)$ with the desired precision ϵ as outlined in Figure 5.

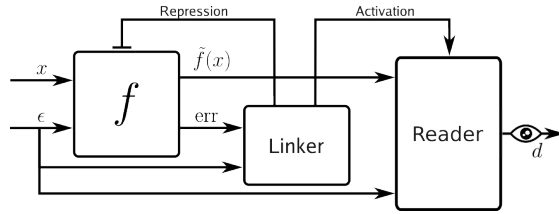
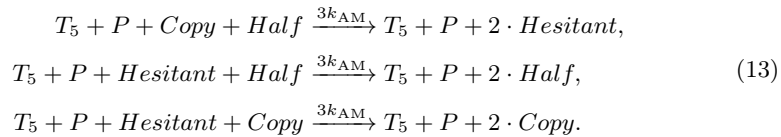


Fig. 5. Schematic figure of a complete analog machine to compute the function f . The first module takes as input x and the desired precision ϵ and outputs a (possibly not computable) value $\tilde{f}(x)$ while also providing its current estimation of the error on err . A linker module halts the computation once the precision is reached and activates a reader module that takes both the output of the previous module and the desired precision and returns a physically observable signal which allows us to construct a dyadic d encoding the result with desired precision.

:w

To reach this precision, we need to have both $\epsilon \geq e^{-k_{\text{exp}}\tau}$ and $\epsilon \geq e^{\frac{-k_{\text{AM}}\tau}{1+\sqrt{2}}}$. We suppose that we are given the precision as a species with a concentration p such that $\epsilon = e^{-p}$. We thus need $k_{\text{AM}} > \frac{3p}{\tau}$ and $k_{\text{exp}} > \frac{p}{\tau}$. To allow the CRN to adapt automatically to the desired precision, the idea is to introduce a catalyst species to tune the rates at which the reactions take place, in order to obtain a satisfying precision. In practice, we may simply use p as the tuning species.

The approximate majority part, for example, would thus become:



And similarly for all the reactions involving k_{exp} and k_{AM} .

To conclude this section on the reader module. The attentive reader may see a contradiction between the quadratic time discussed in sec. 4.1, and the fact that we can adapt to arbitrary precision without modifying the clock in this section (hence achieving a $o(p)$ time). The crucial difference lies in the bounds of the ODE. When adjusting the time of the clock, all the solutions of the ODE are bounded by a constant (2 in practice). While in the reader module, the concentration of the precision species increases with the precision (quite obviously). However, we should also stress that it is unclear how exactly the complexity of the PODE/CRN computation framework can be related to that of conventional computation on a Turing machine, apart from the characterization of the polynomial time complexity class [2].

5 Conclusion

In this paper, we have presented a CRN converter that allows us to read an analog input such as the concentration of a chemical species by displaying its dyadic representation as a series of binary spikes on the concentration of an output species. We also conduct an in-depth analysis of the precision that is theoretically possible to reach with such a device according to the tuning of the three main types of rates that appear in the reaction: the clock k_{clock} , the approximate-majority k_{AM} and the basic operations k_{exp} . In particular, we show that for fixed k_{exp} and k_{AM} adjusting the clock leads to a reading time that increases quadratically with the desired precision while keeping all the concentration within constant bounds.

We thus have contributed to both theoretical questions exposed in the introduction.

Concerning the computation with PODE, we have shown that it is indeed possible to construct a PODE that takes in input a bounded concentration and a desired precision and returns the dyadic encoding of a number approaching the input with the desired precision. Provided that we provide guaranty on the behavior of the clock and the halter module on a formal level, potentially by reasoning on a more complex CRN, and get to wrap everything together, this would validate the computational framework proposed in [6] on a more practical level.

Regarding the Hartmanis-Stearns conjecture, this clarifies the picture. If it is possible to compute the value of an algebraic irrational number in real time, it is actually more difficult to read the output value once the computation has reached a sufficient precision. Indeed, the reader module is either bounded by a constant and quadratic in the precision needed or linear in time but bounded by a variable that scales like the precision. The difficult question to determine how these behaviors may be related to the number of transitions of a multi-tape Turing machine is still pending.

This work could be extended in several directions. The most interesting one would be to replace the clock with a handshaking mechanism. The idea would

be to wait until sufficient precision is reached before launching the next step of the computation. This would allow for a kind of dynamical adjustment of the time spent on the different cycles, going fast when the input is close to 0 or 1 and taking more time when the comparison is difficult.

It is also unclear if this CRN is optimal in terms of time and space complexity for the desired behavior. As this kind of analog framework is relatively new, very few works exist to determine such bounds and even, what are the relevant quantities to look at. In [2], Pouly proposes the length of the solution curve and shows that it allows us to characterize the P-time class. But how it is possible to build other classes of complexity inside the analog computation framework and how to relate them to the ones of the logical complexity is still a field largely unexplored.

Finally, we also start working at the other end of the chain: looking at how we can build a concentration satisfying a desired precision from a dyadic encoding as input. As we try to ensure some form of robustness with respect to the timing and intensity of the spikes, this work is surprisingly more difficult than the one discussed here. But it is in a good way and may be the subject of a short communication in future work.

References

1. Olivier Bournez, Manuel L. Campagnolo, Daniel S. Graça, and Emmanuel Hainry. Polynomial differential equations compute all real computable functions on computable compact intervals. *Journal of Complexity*, 23(3):317–335, 2007.
2. Olivier Bournez, Daniel S. Graça, and Amaury Pouly. Polynomial Time corresponds to Solutions of Polynomial Ordinary Differential Equations of Polynomial Length. In *43rd Int. Colloquium on Automata, Languages, and Programming, ICALP 2016, July 11-15, 2016, Rome, Italy*, volume 55 of *LIPICs*, pages 109:1–109:15. Schloss Dagstuhl - Leibniz-Zentrum fuer Informatik, 2016.
3. Olivier Bournez, Daniel S. Graça, and Amaury Pouly. On the functions generated by the general purpose analog computer. *Information and Computation*, (accepted under minor revision), 2017.
4. Luca Cardelli and Attila Csikász-Nagy. The cell cycle switch computes approximate majority. *Scientific Reports*, 2, 09 2012.
5. François Fages, Mathieu Hemery, and Sylvain Soliman. On biochem symbolic computation pipeline for compiling mathematical functions into biochemistry. *ACM Commun. Comput. Algebra*, 58(2):15–22, January 2025.
6. François Fages, Guillaume Le Guludec, Olivier Bournez, and Amaury Pouly. Strong Turing Completeness of Continuous Chemical Reaction Networks and Compilation of Mixed Analog-Digital Programs. In *CMSB'17: Proc. of the fiveteen international Conf. on Computational Methods in Systems Biology*, volume 10545 of *LNCS*, pages 108–127. Springer-Verlag, September 2017.
7. D.S. Graça and J.F. Costa. Analog computers and recursive functions over the reals. *Journal of Complexity*, 19(5):644–664, 2003.
8. Juris Hartmanis and Richard E Stearns. On the computational complexity of algorithms. *Transactions of the American Mathematical Society*, 117:285–306, 1965.
9. Mathieu Hemery, François Fages, and Sylvain Soliman. On the complexity of quadratization for polynomial differential equations. In *CMSB'20: Proc. of the*

- eighteenth international Conf. on Computational Methods in Systems Biology*, LNCS. Springer-Verlag, September 2020.
10. Mathieu Hemery, François Fages, and Sylvain Soliman. Compiling elementary mathematical functions into finite chemical reaction networks via a polynomialization algorithm for ODEs. In *CMSB'21: Proc. of the nineteenth international Conf. on Computational Methods in Systems Biology*, volume 12881 of *LNCS*. Springer-Verlag, September 2021.
 11. Mathieu Hemery, François Fages, and Sylvain Soliman. A polynomialization algorithm for elementary functions and odes, and their compilation into chemical reaction networks. In *CASC'21: Computer Algebra in Scientific Computing, proceedings of short papers*, September 2021.
 12. C.E. Shannon. Mathematical theory of the differential analyser. *Journal of Mathematics and Physics*, 20:337–354, 1941.
 13. James Thomson. On an integrating machine having a new kinematic principle. *Van Nostrand's Eclectic Engineering Magazine (1869-1879)*, 15(94):301, 1876.
 14. Alan Mathison Turing et al. On computable numbers, with an application to the entscheidungsproblem. *J. of Math*, 58(345-363):5, 1936.
 15. Eberhard O Voit, Harald A Martens, and Stig W Omholt. 150 years of the mass action law. *PLoS computational biology*, 11(1):e1004012, 2015.

A Appendix

A.1 Precision computation

Most differential equations involved in the dyadic converter harbor converging exponential as solutions, that is, functions of the form:

$$f(t) = f_\infty + (f_0 - f_\infty)e^{-k_{\text{exp}}t},$$

where f_0 is the value of the concentration at $t = 0$, f_∞ is the desired steady state, and k_{exp} is the rate constant of the reaction. For model (9), this covers all the reactions for which the rate is set to “rate”.

Thus, if we suppose that the reactions are active for a time larger than τ , the function is stopped at a value closer to f_∞ than: $f_\infty + (f_0 - f_\infty)e^{-k_{\text{exp}}\tau}$, introducing the adimensional quantity $\epsilon = e^{-k_{\text{exp}}\tau}$ we can bound the final value f_τ by (in the case where $f_0 < f_\infty$):

$$f_\tau \in [f_0 + (f_0 - f_\infty)\epsilon, f_\infty] \quad (14)$$

Knowing this allows us to compute the bounds on the value of the different species during the time evolution of one cycle of our converter module as presented in table 2; and at the end, the concentration I_f of the Input species at the end of one clock cycle as a function of its concentration I_0 at the start of the cycle, specifically:

$$\begin{cases} I_f \in [2I_0 - 3\epsilon, 2I_0] & \text{if } I_0 < \frac{1}{2}, \\ I_f \in [2I_0 - 1 - 2\epsilon, 2I_0 - 1 + \epsilon] & \text{if } I_0 > \frac{1}{2}. \end{cases} \quad (15)$$

	Input	Tempo	Copy	Half	Output
Step 0	I_0	0	0	0	0
Step 1	I_0	$[I_0(1 - \epsilon), I_0]$	-	$[\frac{1}{2}(1 - \epsilon), \frac{1}{2}]$	-
Step 4	$[I_0 + I_0(1 - \epsilon)^2, 2I_0]$	$[0, I_0(1 - \epsilon)]$	$[I_0(1 - \epsilon)^2, I_0]$	-	-
Step 5 (O)	-	-	$[0, \frac{\epsilon}{\tau k_{\text{exp}}}]$	$\simeq I_0 + \frac{1}{2}$	-
Step 5 (I)	-	-	$\simeq I_0 + \frac{1}{2}$	$[0, \frac{\epsilon}{\tau k_{\text{exp}}}]$	-
Step 6 (O)	-	-	-	-	$[0, \epsilon]$
Step 6 (I)	-	-	-	-	$[1 - \epsilon, 1]$
Step 7	-	$[0, \epsilon]$	$[0, \epsilon]$	$[0, \epsilon]$	-
Step 8 (O)	$[I_0 + I_0(1 - \epsilon)^2 - \epsilon, 2I_0]$	-	-	-	$[0, \epsilon]$
Step 8 (I)	$[I_0 + I_0(1 - \epsilon)^2 - 1, 2I_0 - 1 + \epsilon]$	-	-	-	$[0, \epsilon]$

Table 2. Bounds on the concentration of the main species of the dyadic converter after the end of the different steps. When needed, we point to the cases where the output species have spiked (I) or not (O). Minus signs indicate that the value does not have changed.

Considering the worst case with an error of order 3ϵ this means that at each step, the value of the Input accumulated an error like: $e_{n+1} = 2e_n + 3\epsilon$, so that

after n steps, the error scales like:

$$e_n = 3(2^n - 1)\epsilon,$$

thus if we still want good precision at step p , this means that we have to impose:

$$\begin{aligned} 3 \cdot 2^p \epsilon &\ll 1, \\ e^{-k_{\text{exp}}\tau} &\ll 2^{-p}, \\ k_{\text{exp}}\tau &\gg p. \end{aligned} \tag{16}$$

Now, reaching step p asks for a time $T(p) = 8\tau p$ as the clock cycle comports eight steps. As we have $\tau \propto p$ by our previous computation, we can conclude that reaching a given precision asks for a time that scales quadratically:

$$T(p) \propto \frac{p^2}{k_{\text{exp}}}. \tag{17}$$

A.2 Convergence of approximate majority

Let us remind the ODEs associated to the model (6):

$$\begin{aligned} \dot{A} &= -k_1 AH + k_2 UA \\ \dot{H} &= -k_1 AH + k_2 UH \\ \dot{U} &= 2k_1 AH - k_2 U(A + H) \end{aligned} \tag{18}$$

The obvious conserved quantity ($A + H + U = C_t$) allows us to introduce the reduced variables: $a = \frac{A}{C_t}$, $u = \frac{U}{C_t}$ and $(1 - a - u)$ as the equivalent for H . We obtain the equations³:

$$\begin{aligned} \dot{a} &= -k_1(a(1 - a - u)) + k_2 ua & a(t=0) &= \alpha \\ \dot{u} &= 2k_1(a(1 - a - u)) - k_2 u(1 - u) & u(t=0) &= 0 \end{aligned} \tag{19}$$

Once again a change of variable is necessary to simplify these equations, we use the variable $\tilde{a} = a + \frac{u}{2}$, giving:

$$\begin{aligned} \dot{\tilde{a}} &= k_2 u \left(\tilde{a} - \frac{1}{2} \right) \\ \dot{u} &= 2k_1 \left(\tilde{a} - \frac{u}{2} \right) \left(1 - \tilde{a} - \frac{u}{2} \right) - k_2 u(1 - u) \end{aligned} \tag{20}$$

Supposing that $k_1 \gg k_2$ allows us to approximate u as a fast variable with the equilibrium given by:

$$u = \left(\sqrt{4\tilde{a}(1 - \tilde{a}) + 1} - 1 \right), \tag{21}$$

³ To be exact, we should also replace k_1 and k_2 by their rescaled version $\tilde{k} = kC_t$, we omit this detail for the sake of readability.

that we can plug in the equation of \tilde{a} . As this equation is separable, we obtain the relation:

$$k_2 t + c_1 = -\log(\sqrt{s} - 1) - \log(\sqrt{s} - 2\tilde{a} - 1) + (1 + \sqrt{2}) \log(\sqrt{s} - 2\sqrt{2}\tilde{a} + 2\tilde{a} - 1) - (\sqrt{2} - 1) \log(\sqrt{s} + 2(1 + \sqrt{s})\tilde{a} - 1) = f_i(\tilde{a}) \quad (22)$$

where for readability, we denote: $\sqrt{4\tilde{a}(1 - \tilde{a}) + 1} = \sqrt{s}$ and c_1 is an integration constant that should be computed from the initial condition. The function f_i is symmetrical under the relation $\tilde{a} \rightarrow 1 - \tilde{a}$ and describes the evolution of the system over time. That is, if we want a final value r while starting at \tilde{a}_0 , we have to wait for a time: $t = \frac{f_i(r) - f_i(\tilde{a}_0)}{k_2}$. In our case, we have a fixed time τ a precision requirement r and want to determine how close we can be to one half to still reach it. That is, we want to know δ such that:

$$k_2 \tau = f_i(r) - f_i\left(\frac{1}{2} - \delta\right).$$

An expansion around both $r \ll 1$ and $\delta \ll 1$ gives us:

$$\begin{aligned} k_2 \tau &= -\log 4r^2 - (1 + \sqrt{2}) \log \delta \\ \log \delta &= -\frac{\log 4r^2}{1 + \sqrt{2}} - \frac{k_2 \tau}{1 + \sqrt{2}} \end{aligned} \quad (23)$$

From this, we can estimate the scaling of the critical threshold, below which the approximate majority is not able to discern the majority species as a function of k_2 and τ :

$$\delta^* \propto \exp -\frac{k_2 \tau}{1 + \sqrt{2}}. \quad (24)$$

All this derivation has been done under the assumption that $k_1 \gg k_2$ which is the most natural one. To be complete, suppose that $k_1 \ll k_2$. We can easily prove that, once again, u equilibrates quickly near 0 giving us: $u = \frac{2k_1}{k_2} \tilde{a}(1 - \tilde{a})$ and inserting it in the equation over \tilde{a} we have:

$$\dot{\tilde{a}} = 2k_1 \tilde{a}(1 - \tilde{a})\left(\tilde{a} - \frac{1}{2}\right). \quad (25)$$

In this simpler case, we have the analytical solution:

$$\tilde{a}(t) = \frac{4e^{c_0} + e^{k_1 t} \pm \sqrt{4e^{c_0 + k_1 t} + e^{2k_1 t}}}{2(4e^{c_0} + e^{k_1 t})}, \quad (26)$$

where c_0 is the integration constant that can be derived from the initial condition. The two important elements to remark are that the \pm sign depends on whether α is initially higher or lower than one half and that the system follows the same kind of sigmoidal pattern as previously, starting by a slow phase to escape the

intermediate region followed by an exponential convergence toward one of the two attractors that are 0 and 1.

From this, we can derive the same kind of relation as previously:

$$\delta^* \propto e^{-\frac{k_1 \tau}{2}}.$$

A.3 Integrating over a cosine

We approximate the sine wave of our clock by square signal to ease the analysis. Actually, we can pretty easily compute the equivalent of our $\epsilon = \exp -\tau k_{\text{exp}}$ quantity for a sinusoidal wave of frequency ω .

Let us use the activator species T to activate two reactions, thus creating a simple steady state for the molecule R (for reporter): $T \xrightleftharpoons{k_{\text{exp}}} T + R$ and use a sinusoidal profile:

$$T(t) = \begin{cases} \sin t\omega\pi & \text{if } t \in [0, \omega^{-1}] \\ 0 & \text{otherwise} \end{cases} \quad (27)$$

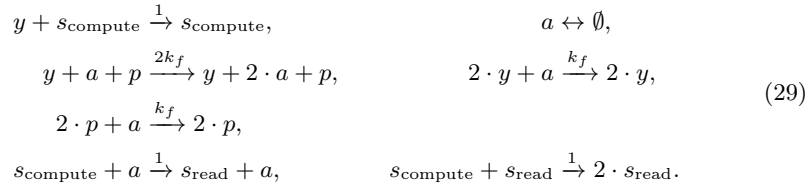
The associated ODE is: $\dot{A} = k_{\text{exp}}T(1 - A)$ that is separable, and thus we easily obtain:

$$A_{\infty} = 1 - e^{-\frac{2k_{\text{exp}}}{\omega\pi}} = 1 - \epsilon. \quad (28)$$

Hence, in our case where $\omega = \pi^{-1}$, we simply have $\epsilon = e^{-2k_{\text{exp}}}$ where k_{exp} is the rate constant of the main reaction of the current step. Or said otherwise, the sine wave is equivalent to a square signal of duration $\tau = 2$.

A.4 Linker CRN

The following CRN presents a prototype of linker CRN that allows to use our reader CRN on the output of a computing CRN as presented by Fages et al. Here, y is the species mimicking the precision of the main CRN, a is an activator that spikes when the desired precision p is reached. Finally, s_{compute} and s_{read} represent the two species of the switch that turns the whole CRN from computing to reading mode by catalyzing every reactions in their respective parts.



With at $t = 0$, $s_{\text{compute}} = 1$ and $a = 1$.